

Research Journal of Pharmaceutical, Biological and Chemical Sciences

Comparative Study of the Skeletogenesis of Limb Autopods in the Developing Chick *Gallus domesticus* and Toad *Bufo regularis*

Gamal M Badawy*, Saber A Sakr, and Marwa N Atallah

Department of Zoology, Faculty of Science, Menoufiya University, Egypt.

ABSTRACT

Limb development is an excellent model for studying how patterns of differentiated cells and tissues are generated in vertebrate embryos. The present descriptive study deals with the skeletogenesis of limb autopods using certain relevant stages from two different experimental models, i.e. the chick *Gallus domesticus* and the tadpole *Bufo regularis*. The study comprised anatomical description of skeleton development including chondrogenesis and the appearance of ossification centers during certain embryological stages. In order to analyze the ontogenetic patterns of skeletogenesis of limb autopods, both single and double transparency techniques were adopted utilizing Alcian blue and Alizarin Red S stains. The chronological order of both chondrogenesis and endochondral ossification was therefore investigated. Although the former occurred at the same stage in both limbs, the latter of the hindlimb lags behind its counterpart in the chick forelimb by one stage. In the developing tadpole stages, digits appear sequentially as outgrowths from the limb palette. It is therefore proposed that mesenchymal cells migrate from the interdigital spaces to the digits in the developing toad. This difference in the mode of digit formation points to the possibility of different origin of limbs in both models. However, the developing limb of both models followed a general proximo-distal progression and a postaxial polarity in digit development which occurred in a postero-anterior direction. Morphological figures, supplemented by histological micrographs, are presented to describe the skeletogenesis of limb autopods.

Keywords: Embryogenesis; Limb development; Skeletogenesis; Autopodium; *Gallus domesticus*; *Bufo regularis*

*Corresponding author

INTRODUCTION

Limb development has been a classic model to study pattern formation during embryonic development since it constitutes an amenable system to analyze how a group of undifferentiated cells give rise to a complex anatomical structure [1-4]. Basic cellular activities such as cell proliferation, differentiation, cell death or intercellular signaling take place during limb bud initiation and outgrowth and the interplay between all of these cellular behaviors together with the genetic history of cells (lineage) will lead to the formation of specific structures at precise locations. Vertebrate limbs develop from small buds of apparently homogenous population of undifferentiated mesenchyme cells, mostly derived from the lateral plate mesoderm, encased in ectoderm [5]. These buds continue to elongate from the body wall and later begin to take on a limb-like shape with a broad region at the tip of the limb where the digits will form. At the same time as the bud is elongating, mesenchyme cells in the base of the bud, the part nearest the body wall, start to differentiate to lay down the pattern of the specialized tissues of the limb, e.g. the skeleton, while the mesenchyme cells at the tip of the bud remain undifferentiated [6, 7].

During vertebrate limb development, epithelial-mesenchymal interactions are crucial for the emergence of limb buds and the core of this process is the establishment of a reciprocal loop based on fibroblast growth factors; (FGFs) signaling [8]. The patterning of limb mesenchyme is therefore due to interactions between the mesenchyme and the overlying epithelium [2]. The embryonic limb possesses two signaling centers, the apical ectodermal ridge (AER) and the zone of polarizing activity (ZPA), which produce signals responsible for directing the proximo-distal (PD) outgrowth and antero-posterior (AP) patterning, respectively [9, 10]. As specialized thickening of the ectoderm, the AER plays crucial roles during development producing secreted signalling molecules that act on underlying mesenchyme cells to control growth and patterning [11-16]. The maintenance of the AER and/or production of these signalling molecules in the ectoderm, in turn, are influenced by secreted signalling molecules produced by the mesenchyme. Limb bud outgrowth is accompanied by the successive laying down of structures along the PD axis [17, 18].

Despite considerable recent advances in our understanding of how limbs develop (reviewed in [19]), a major unresolved question is how the positional information that cells acquire at early steps of limb bud outgrowth is translated into anatomy at later stages, to form the complex array of tissues with distinctive morphological and functional characteristics that constitutes a limb. Another important question that has not been addressed is how a limb stops growing after all pattern formation has taken place and is then finished with the formation of digits. Tetrapods exhibit great diversity in limb structures among species and in differences between fore- and hindlimbs within species, which typically are correlated with modes of locomotion and life history [6, 20]. These differences are not restricted to mammals but characterize tetrapods as a whole, as evidenced when considering a bird or a frog or a turtle [18]. Variations in limb morphology generally involve elongation, reduction or fusion of skeletal elements [21]. In spite of such variation, there is a conserved, underlying morphology consisting of a single proximal element (stylopod: humerus/femur), paired elements distal to this (zeugopod: ulna/radius, tibia/fibula) and variable numbers of most distal elements of the hand and foot (autopod) including the carpals/tarsals metacarpals/metatarsals of the wrist/ankle, and phalanges of the digits [20]. All vertebrate limbs have, therefore, a similar

structure composed of three proximal-to-distal segments: the stylopod, the zeugopod, and the autopod [22, 23]. While the proximal two limb segments exhibit relatively little variation across tetrapods, the autopod is highly variable [20, 24, 25]. In addition to this PD asymmetry there are conserved postero-anterior (PA) and dorso-ventral (DV) asymmetries. Distally, the pattern terminates in tapered, bilaterally symmetrical digits that vary in number and complexity; however, the peripheral digits are shorter and contain fewer elements than the central digits [21]. In addition to the anatomy of the adult limb, several features of developing limbs are also highly conserved. The skeletal elements generally differentiate in a PD sequence, and there are conserved patterns of "connectivity" between the various skeletal elements [17, 18, 26, 27].

The elements of the limb skeleton are laid down in sequence with the structures nearest the main body axis such as humerus/femur of the forelimb/hindlimb forming first, and digits at the tip last [20, 22]. Two steps can be distinguished during the formation of cartilage elements [27, 28]: initial condensation of mesenchymal cells to form prechondrogenic aggregates, where changes in the morphology, shape and adhesion properties of cells occur, and subsequent differentiation of these aggregates into chondrocytes that produce specific extracellular matrix components [23, 28]. Later on, the cartilage template is replaced by bone through an endochondral ossification process [26, 29]. The process of endochondral ossification involves terminal differentiation of chondrocytes to the hypertrophic phenotype, cartilage matrix calcification, vascular invasion, and ossification [30-33]. The cellular and molecular mechanisms that control limb morphogenesis are still largely mysterious, although morphogenesis is the most obvious and important task of development [16].

In amniotes and anurans, skeletogenesis generally proceeds in a PD direction and commences with the condensation of the stylopodium [21, 34]. The zeugopodial elements arise as a y-shaped condensation at the distal end of the humerus/femur with the preaxial element usually lagging behind the postaxial one. A number of further condensations establish the proximal elements of the carpus and tarsus. Finally, the distal carpals/tarsals, metacarpals/metatarsals and associated digits are formed, starting with the penultimate, postaxial digit (digit IV in a pentadactyl autopodium) and progressing preaxially in the order IV-(V)-III-II-I. Digit V often arises somewhat independently of the digital arch, although a connection to the remainder of the digital arch exists in some taxa. This characteristic pattern of postaxial dominance has been observed in all of the studied anurans and amniotes with surprisingly little variation in the basic progression of events, given the great morphological and functional diversity of tetrapod limbs [35, 36].

The problem of how digit pattern arises has been tackled by applying the concepts of positional information [37]. According to these concepts, pattern formation is a two step process; in the first step, cells are informed of their position in the limb bud, as a result, they acquire a positional value that encodes this information; in the second step, cells then interpret this information leading to the formation of the appropriate structure at that position. It was therefore proposed that cell position in the limb bud would be specified in relation to the three main axes, PD, PA and DV and positional information across the AP limb axis is provided by signalling of the polarizing region at the posterior margin of the early limb bud [38]. By this time, the small bud has grown substantially and changed shape so that the main regions of the future limb can be made out. However, experiments on chick embryos have shown that cells are specified to form limbs, long before any buds are visible, and that both the AP and the DV

polarity of the limb are already established [39]. During the PD patterning of limbs, digits are the last elements to be laid down [6]. Digits are established as chondrogenic condensations that form in the autopod along the PA axis and are separated by interdigital spaces. The sequence of condensation is characteristic and in most cases begins with the penultimate posterior digit, followed by a PA progression. An exception to this general pattern is condensations in urodeles, where anterior digits condense first, progressing then in an anterior to posterior sequence [26]. One can distinguish different stages in the formation of digits: initial condensation; elongation and segmentation; and finally tip formation [24, 39]. Initially, the regions of the autopod that will make the condensations (digital rays) are defined in contraposition to those that will form the interdigital spaces. This will determine the different outcome of cells in both regions, since condensations will progress to make cartilage, whereas interdigital cells ultimately will die by apoptosis [25, 40, Badawy et al., in preparation].

Digit identity can be defined as the type of digit that develops in a particular position. The collective morphological features of a digit that make it distinct from others are the overall length and especially the number of phalanges and their morphology. In mouse and human both fore- and hindlimbs have five digits, and it is easy to distinguish the most anterior (digit I) and posterior (digit V) from the others. However, it is more difficult to assess the identity of the three middle digits, since all of them have three phalanges and a similar size and shape. Chicken limbs have long been used as a model system in experimental embryology, mainly because of the accessibility to chirurgic manipulations. Another reason for their use in patterning studies is precisely that digits can be easily distinguished, both in wings and in legs. The chicken wing has only three digits that are morphologically very different. From anterior to posterior, digit II has two phalanges, digit III has two and digit IV has only one. (Nomenclature of wing digits as II, III, and IV is the standard used in developmental biology based on embryological data, although the identity and homology of digits in the wing from an evolutionary perspective is a long-standing controversy [41-44]. Also, the number of phalanges in wing digits has been debated [39].

The aim of the present study was to provide a detailed description for both chondrogenesis and osteogenesis during the ontogenetic development of the autopodium of two different experimental models, namely the chick *Gallus domesticus* and the tadpole *Bufo regularis*. To achieve this target, a combination of single and double staining transparency techniques using Alcian Blue (AB) and Alizarin Red S (ARS) were adopted. Furthermore, additional histological investigation has been carried out in order to shed more light on the anatomical structure of the autopod in both models in terms of skeletogenesis.

MATERIALS AND METHODS

ANIMALS AND HUSBANDRY

All the experimental aspects of this work were conducted in compliance with the institutional guidelines for the care and use of animals and approved by the Animal Research

Ethics Committee at Faculty of Science, Menoufiya University. Two, avian and amphibian, experimental models, namely, the chick *Gallus domesticus* and the tadpole *Bufo regularis* were utilized as representative of tetrapods. For investigating the skeletogenesis of chick limb autopods, normal fertilized hen eggs, of a local strain were obtained from a local breeder at Shebeen Elkoom, Menoufiya, Egypt. Before incubation at 37°C temperature and 65% humidity in an artificial incubator, eggs were cleaned with distilled water followed by 70% Ethanol. The eggs were put horizontally and turned over, at least, three times a day. For detailed analysis of the development of chick limb autopods in terms of its morphological and skeletogenesis aspects, a number of developmental stages were selected based on the normal table of Hamburger and Hamilton [45] conducted specifically for chick embryo. After careful morphological investigation, it was clearly appropriate to start staging after 108 hour of incubation, i.e. stage 25 which marks the beginning of autopod specification and end at the post-hatching stage 46. Ten specimens per each selected developmental stage were utilized and therefore, a total of 220 chick embryos were investigated.

For obtaining tadpoles, several ribbons of fertilized eggs or sometimes newly hatched spawns of the toad, *Bufo regularis* were brought into the laboratory from the fields of Shebeen El-Koom districts during the breeding season which lasts from March to September. Developing eggs were collected in a mesh-collecting basket and shipped in plastic bags filled with de-chlorinated tap water. The ribbons were divided into small bunches and kept in white enamel-coated pans provided with two liters of de-chlorinated tap water with sufficient supply of de-chlorinated tap water. De-chlorination was carried out by keeping the ordinary tap water in large uncovered vials in an aerated place, at least overnight. From the initiation of feeding until the end of the aquatic period of development, throughout the study, tadpoles were fed *ad libitum* either freshly or frozen boiled spinach until the beginning of the metamorphic climax phase (stage 59) at which the animals stopped feeding until reaching stage 66. Rearing water was changed every necessitation that was at least once weekly. Starting from stage 56, tadpoles were transferred into other pans with shallower level of water and small pieces of stones. When the second forelimb emerged (stage 59) and following changing-over to air breathing, tadpoles were removed from the pans and housed individually in a labeled bowl with cover and provided with a piece of moistened cotton on the floor. Development was monitored until the tail bud had completely absorbed i.e. reaching the post-hatching stage 66. Rearing took place at room temperature that was 28 ± 2 °C. To trace and describe the morphological and skeletal aspects of limb autopods development, a number of developmental stages were selected based on the normal table of Sedra and Michael [46] which is specific for *Bufo regularis*. Thus, 20 specimens per each selected developmental stage from 53 to 66 were investigated. The histological investigation was restricted to stages 53, 54, 55 & 56. A total of 280 tadpole larvae were investigated.

SAMPLING AND MANIPULATION OF CHICK EMBRYO LIMBS

At the appropriate times for staging according to the normal table of Hamburger and Hamilton [45], eggs were windowed following the protocol of Korn and Cramer [47]. Briefly, the egg was put horizontally and kept in position for two minutes, so that the embryo is located mid-dorsally, and a piece of cello tape, 2 cm x 2 cm, was placed on the egg surface. A small hole was made over the tape via the tip of fine forceps, piercing the egg shell. Using a scissor, the egg shell was cut starting from the hole and carefully guiding the lower blade of the scissor into

the egg with the tips up against the inside of the shell and slowly cutting the shell in a counter-clockwise direction until reaching the initial hole. Thereafter, the cut egg shell was removed carefully so that a window has been made. The albumen and yolk were then poured off and the chick embryo was taken out of the egg into a Petri dish and washed several times with avian saline (0.75 % NaCl). The extra-embryonic membranes were carefully removed in order to have free access to the limbs. Chick embryos of the investigated developmental stages were anesthetized wholly in Ether for 30 min. and then moved to 10 % formalin for an hour. The limbs were isolated and fixed in 10 % formalin for 24 hours. For each stage, ten embryos were fixed in 10 % formalin, washed under running tap water for 12 hours and then stored in 70 % Ethanol until further processing. As a part from the morphological investigation, both limbs as well as the whole embryos of each concerned stage were photographed using either mobile camera fixed on a dissecting binocular microscope in case of early developmental stages or a Nikon Dlx digital camera in case of late developmental stages.

SAMPLING AND MANIPULATION OF TADPOLE LIMBS

For early developmental stages where the forelimb is still concealed by the skin of the operculum (53 – 58), isolation of the forelimbs has been achieved using dissecting binocular microscope. A small Petri dish filled with solid paraffin wax was used to fix the tadpole during the surgical procedure. The animal was placed with abdomen up and held up in position by an entomological pin passing vertically through the tail, just near the cloacal aperture, and another one in the head. Irredecomy scissor was carefully used to make a longitudinal cut in the abdominal wall from the base of the abdomen up to the head, then with the help of a fine tipped forceps, the gut and most internal organs were removed. The fore limbs were isolated from both sides, just below the gill chambers, where they are ensheathed in a heavily pigmented membrane. Limb specimens were fixed and processed as mentioned before. Tadpoles and their corresponding limbs were photographed as mentioned for chick embryos.

SKELETAL PREPARATIONS

Three different transparency techniques were employed to investigate the developing skeletal structure of both chick and toad using AB and ARS for staining cartilage and bone respectively. To achieve this target, the whole range of the investigated developmental stages was divided into three sets. The first set of specimens was stained with AB alone for demonstrating cartilage, the second set was stained with ARS alone for demonstrating bones and the third set was subjected to double staining using both AB and ARS. In order to avoid unnecessary repetition, the second set of specimens was not presented in the results section. Several methods have been tried without getting satisfactory results and therefore, it was necessary to add some modifications to the original methods as following:

A) Demonstration of cartilage using AB (modified from Cortés-Delgado, et al. [48]) where specimens were:

- 1- Fixed in 10 % formalin, washed under running tap water for 12 hours and then preserved in 70 % Ethanol.
- 2- For toad, limbs were de-pigmented by adding 30 to 40 drops of H₂O₂ in 10 ml 70 % Ethanol depending on the considered developmental stage.

3- Transferred to 95 % Ethanol for 24 hours.

4- Stained in a freshly prepared mixture of :

- 10 mg AB
- 80 ml 95 % Ethanol
- 20 ml Glacial acetic acid

At 28 ± 2 °C for 24 hours.

5- Transferred to two changes of 95 % Ethanol for two hours each.

6- Rehydrated for six hours in successive changes of 70 %, 50 % Ethanol and distilled water.

7- Immersed for 8 hours in a solution of 30 ml saturated sodium borate and 70 ml distilled water.

8- Transferred to several changes of KOH solution until completely transparent.

9- Transferred to an equal mixture of KOH solution and Glycerol for 30 min. and finally stored in pure Glycerol.

B) Demonstration of bone using ARS (modified from Pramod, et al. [49]) where specimens were:

1- Processed following steps 1 to 3 as mentioned in method A.

2- Transferred to several changes of KOH solution until completely transparent.

3- Stained in a freshly prepared mixture of 3 mg ARS in KOH solution for 48 hours at room temperature 28 ± 2 °C.

4- Transferred to two changes of KOH solution to get rid of excess stain.

5- Transferred to successive changes of KOH solution and Glycerol as follows:

- 8: 2 KOH solution: Glycerol 30 min.
- 5: 5 KOH solution: Glycerol 30 min.
- 3: 7 KOH solution: Glycerol 30 min.

6- Stored in pure Glycerol.

C) Demonstration of the whole skeletal structure by double staining using both AB and ARS (modified from Cortés-Delgado, et al. [48]) where specimens were:

1- Processed following steps (1) to (8) as mentioned in method (A).

2- Stained in 3 mg ARS in KOH solution for 48 hours at room temperature 28 ± 2 °C.

3- Transferred to KOH for an hour and changed until the solution was clear.

4- Transferred to an equal mixture of KOH solution: Glycerol for 30 min. and stored in pure Glycerol.

In all steps, KOH solution was applied with two concentrations i.e. 2 % for chick embryos and 0.5 % for tadpoles.

Specimens were examined in Glycerol at low resolution under Heerbrugg M3C dissection microscope and at high resolution using a Leitz Laborlux S light microscope. Photographs of the representative samples were taken using a Nikon Dlx digital camera and edited using PhotoShop 7.0 (Adobe Systems, San Jose, CA).

HISTOLOGICAL EXAMINATION

The fixed limb autopods of 25 – 35 chick developmental stages and 53 to 56 tadpole developmental stages. The autopodium of chick developmental stages 34 and 35 were decalcified by immersion in 2 % nitric acid for a period of four and six days respectively. However, stages before 34 were processed without decalcification. All specimens were transferred to 70 % Ethanol for 30 min, dehydrated, cleared, embedded, oriented and blocked out in paraffin wax in embryo dishes under dissecting binocular microscope in order to produce longitudinal sections. Five μm thick serial longitudinal sections were produced using a rotary microtome. Histological staining was performed with Mallory Triple Stain (MTS). However, tadpole stages were embedded in resin and stained with Toluidine Blue (TB). For histological procedures see [50].

CELL DENSITY ANALYSIS

The cell density in the developing autopods of the toad of stages 53, 54, 55 and 56 were determined by counting the total number of nuclei per unit length in the digital and interdigital areas using square eye piece micrometer. Sex specimens were examined at each developmental stage, and the mean values and standard error of the mean (SEM) were calculated. This has been done by using semithin sections stained with TB. Because of similarity, data obtained from counting cell density in the forelimb were only presented to avoid unnecessary repetition

STATISTICAL ANALYSIS

Data obtained from investigating the cell densities were expressed as mean \pm SEM. The data were analyzed statistically for normal distribution (student's test) and homogeneity of variances (Levene test) using statistical program of social sciences (SPSS) software for windows, version 11. Differences were considered significant at $P<0.05$. The significances of the obtained data were classified into three categories i.e. $P<0.0001$, $P<0.03$ and $P<0.05$.

RESULTS

Figure (1) shows the morphological features of part of the selective developmental stages of the chick embryos used in the present study. Progressive morphological differences among the developmental stages are evident in terms of both the embryos as a whole and the limbs. As the figure demonstrates, stage 25 (Fig. 1 A) constitutes the first developmental stage considered in terms of limb development where the autopodium can be recognized but no demarcation of digits can be seen. In contrast, the developmental stage 36 (Fig. 1 L) has an autopodium with the complete set of digits regardless of the ossification process which has been dealt with for all investigated developmental stages within the present study.

General morphology of part of the utilized tadpole developmental stages including limb detail is provided in Fig. 2. These developmental stages started with the stage 53 where the autopodium is flattened without a clear sign of interdigital indentations (Fig. 2 A) and ended with stage 56 which is characterized by the presence of a complete set of digits with clear indentations (Fig. 2 D) regardless of the ossification process. In these four developmental

stages, the forelimb was isolated surgically from the body as it is concealed by the skin of the operculum.

Investigating the chondrogenesis of the developing forelimb of chick embryos revealed that a Y-shaped condensation has appeared indicating the radius and ulna at stage 25 (Fig. 3 A). Stage 26 (Fig. 3 B) witnessed the very early indication of the appearance of separate condensations which will consequently form each of the three digits that characterized the avian wing in a PA sequence. During the subsequent stages, progressive development of the chondrogenesis as well as the segmentation of the cartilage within the digit rays which were joined by colorless soft tissue (Figs. 3 C-I). As the Figure indicates, the process of chondrogenesis processed in a PD direction, i.e. distal carpals, metacarpals and phalanges. The pattern of the onset of ossification, as seen in whole mounts stained with ARS, started at stage 34 (Fig. 4 A) and ended at the post-hatching stage 46 (L) is provided in Fig. 4. The Figure demonstrates the chronological order of appearance of ossification centers in the skeletal elements of the developing wing. Stage 34 (Fig. 4 A) showed no sign of ossification in the autopodium and the first segment to ossify in the autopodium was the metacarpal of the third digit of stage 35 (Fig. 4 B). Regardless of the increase in the ossification process, this situation persisted until stage 39 (Fig. 4 E). The metacarpal of the fourth digit ossified at stage 40 (Fig. 4 F). Starting from stage 41, ossification of the phalanges began in the third digit (Fig. 4 G). The metacarpal of the second digit began to ossify at stage 42 with the appearance of the second ossified centre in the third digit (Fig. 4 H). The following developmental stages, i.e. 43-46 displayed a gradual and progressive degree of ossification (Fig. 4 I-L).

In the developing chick leg, developmental stages 25 and 26 displayed no signs of chondrogenesis in the autopodium (Fig. 5 A & B). Tracing the process of chondrogenesis revealed that it followed a PD direction i.e. distal tarsals, metatarsals and phalanges of the toes. Condensations that will form each of the four toes arise at stage 27, again in a PA sequence (Fig. 5 C). Digital rays start off as continuous rods of cartilage that elongate and periodically segment to form interphalangeal joints and thus generate a precise number of phalanges. This has been done progressively in a PD direction (Fig. 5 C-J). Some specimens at stages 30 (Fig. 5 F) and 32 (Fig. 5 H) displayed a forked first toe through the presence of a transient cartilaginous element which disappeared at stage 33 (Fig. 5 I). The pattern of the onset of ossification as seen in whole mounts stained with ARS from stage 35 (Fig. 6 A) for all the skeletal elements of the limb up to the post-hatching stage 46 is presented in Fig. 6 I. The Figure demonstrates the chronological order of appearance of ossification centers in the skeletal elements of the developing limb. From the developmental stage 35 (Fig. 6 A) until stage 40 (Fig. 6 D), only the metatarsals were ossified in the autopodium. Stage 41 witnessed the starting of ossification of the phalanges of toe IV, III and II with no sign of ossification in the phalanges of the first toe (Fig. 6 E). The ossification of phalanges went progressively in the next stages (Fig. 6 F-I)

As Fig. 7 shows, the cartilaginous skeletal elements of the autopodium of tadpole forelimb are laid down sequentially in a PD direction as development proceeds. The process of chondrogenesis of the autopodium displayed its first indication of appearance at stage 55 (Fig. 7 A). At the subsequent stage i.e. stage 56, the process of chondrogenesis became evident distally in the autopodium (Fig. 7 B). The pattern of the onset of ossification as seen in whole mounts stained with ARS starting from stage 57 (Fig. 7 C) and ending with the developmental stage 65 (Fig. 7 J) is provided in Fig. 7 (C-J). The phalanges began the ossification process at

stage 59 with the metacarpals of digits IV, III and II (Fig. 7 E). The ossification of phalanges went progressively in a PD direction with the advancement of the developmental stages as expressed by the intensity of the ARS stain. Starting from the developmental stage 60 (Fig. 7 F) and ending with stage 65 (Fig. 7 J). Regardless of the elongation of the developing phalanges, the phalangeal formula of the forelimb showed the same numbers, i.e. 2, 2, 3 & 3 for digits I, II, III, & IV respectively. Additionally, all the osseous elements of the developmental stages 64 & 65 displayed an advanced stage of ossification.

Development of cartilage in the autopodium of the hindlimb was first seen at stage 54 in the site of the prospective astragulus and calcaneum (Fig. 8 A). The subsequent two stages, i.e. 55 and 56 displayed more pronounced chondrogenesis in a PD direction (Fig. 8 B & C). At stage 57 (Fig. 8 D), the first ossified centers in the autopodium appeared proximally in the astragalus and calcaneum. Ossification of the metatarsals as well as the proximal phalanges began at the developmental stage 58 but became more pronounced at stage 59 (Fig. 8 E). From the developmental stage 60 (Fig. 8 F) until stage 65 (Fig. 8 J), the phalangeal formula showed no change in terms of numbers, i.e. 2, 2, 3, 4 & 3 for toes I, II, III, IV & V respectively. However, in terms of the degree of ossification, these skeletal elements exhibited more darkly stain progressively with the developmental stage (Fig. 8 F-J).

Histological investigation of the serial longitudinal sections in the autopodium of forelimbs of the selective chick developmental stages confirmed the whole mount transparency investigation and revealed that the first sign of cartilage condensation in the autopodium appeared at the developmental stage 26 (Fig. 9 A). This condensation occurred in a PD direction, i.e. in the area of distal and metacarpals then went distally in the sites of the prospective phalanges (Fig. 9 A-C). Developmental stages from 30 onwards witnessed the beginning of cartilage hypertrophy (Fig. 9 D-H). Fig. (10 A & B) demonstrates the AER which was pronounced at stage 25 where the limb is consisting of an apparently homogenous population of undifferentiated mesenchymal cells, associated with the primitive capillary network and encased in the ectoderm. At the subsequent stage, i.e. 26 there was an early aggregation for the mesenchyme cells in the proximal part of the autopodium (Fig. 10 C) and in accordance with the whole mount investigation, stage 27 (Fig. 10 D) witnessed the evident chondrification of the autopodium in a PD direction in terms of the whole limb but in a PA direction in terms of digitation. The developmental stages up to stage 33 (Fig. 10 E-K) displayed more progressive histological differentiation of the autopodium in a PD direction.

In the autopodium of the forelimb of the tadpole stage 53 (Fig. 11 A), the AER has disappeared and the mesenchyme condensation was evident in the whole limb in a PD direction in terms of the limb and in a PA direction in terms of the process of digitation. The autopodium of the forelimb of stage 56 (Fig. 11 B) displayed a pronounced chondrogenesis in accordance with the mesenchyme condensation seen the previous developmental stages in a clear agreement with the whole mount investigation i.e. in a PD direction in terms of the limb and in a PA direction in terms of digitation. Except differences in the numbering of the developmental stages as well as number of digits, the autopodium of the hindlimb exhibited the same trend displayed in the autopodium of the forelimb. This can be noticed in Fig. 11 C (stage 55) and Fig. 11 D & E (stage 56).

Fig. 12 and Table (1) show the determination of cell densities in both digital and interdigital areas in the developing forelimb autopodium of the toad. The two illustrations demonstrate that cell density was comparatively high in the digital areas and progressively decreased with the advancement of the developmental stage owing to the condensation in the early stages and hypertrophy of cartilage cells in the later stages.

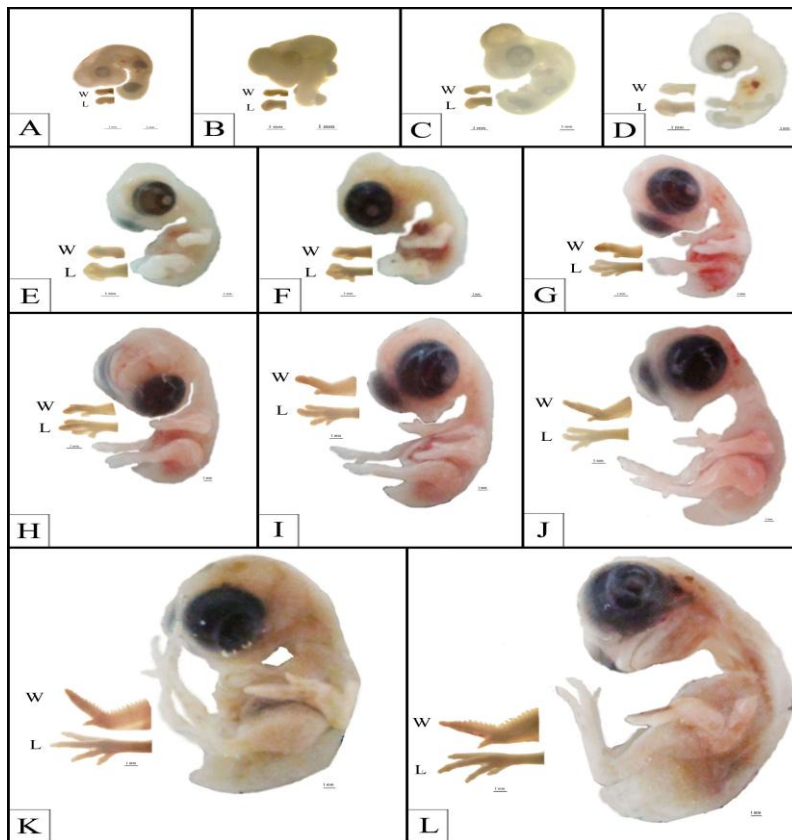


Figure 1: Lateral view photographs of gross morphology of chick embryos, including limb detail, at stages 25 – 36 (A – L). L, Leg; W, Wing. Scale bar = 1mm.

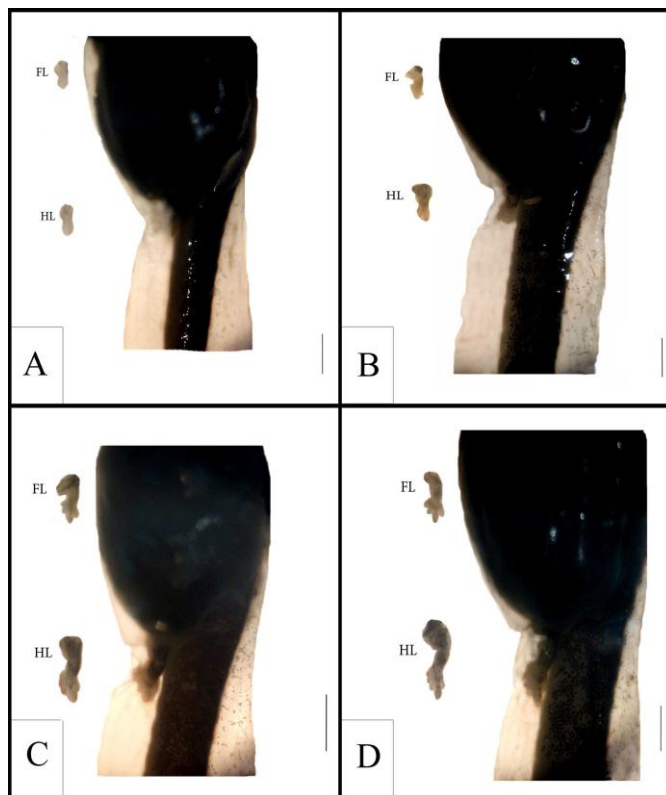


Figure 2: Lateral view photographs of gross morphology of tadpole larvae including limb detail, at stages 53 – 56 (A – D). FL, Forelimb; HL, Hindlimb. Scale bar = 1mm.

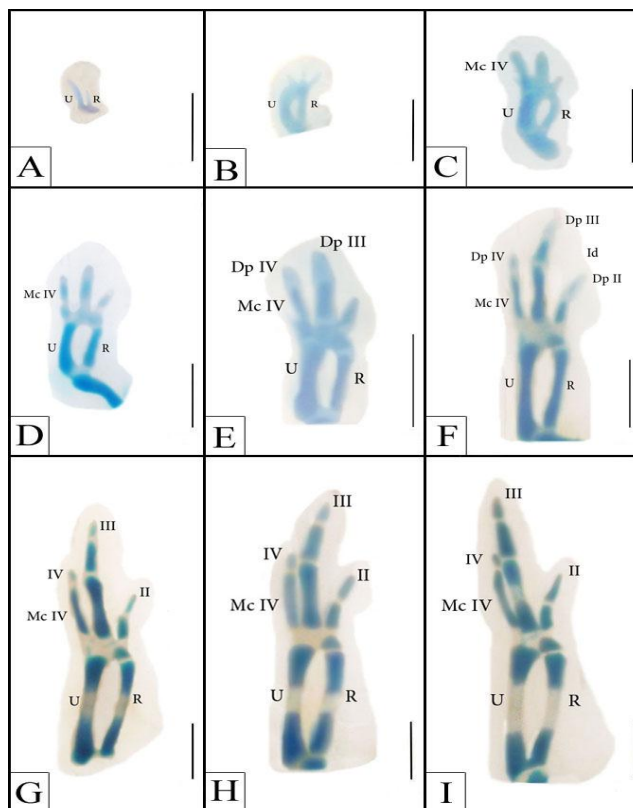


Figure 3: Series of Alcian Blue - stained chick forelimb distal cartilaginous elements at stages 25 – 33 (A-I). Dp II-IV, Digit primordia II-IV respectively; Id, Interdigital space; II-IV, Digits II-IV respectively; Mc IV, Metacarpal IV; R, Radius; U, Ulna. Dorsal view. Scale bar = 1mm.

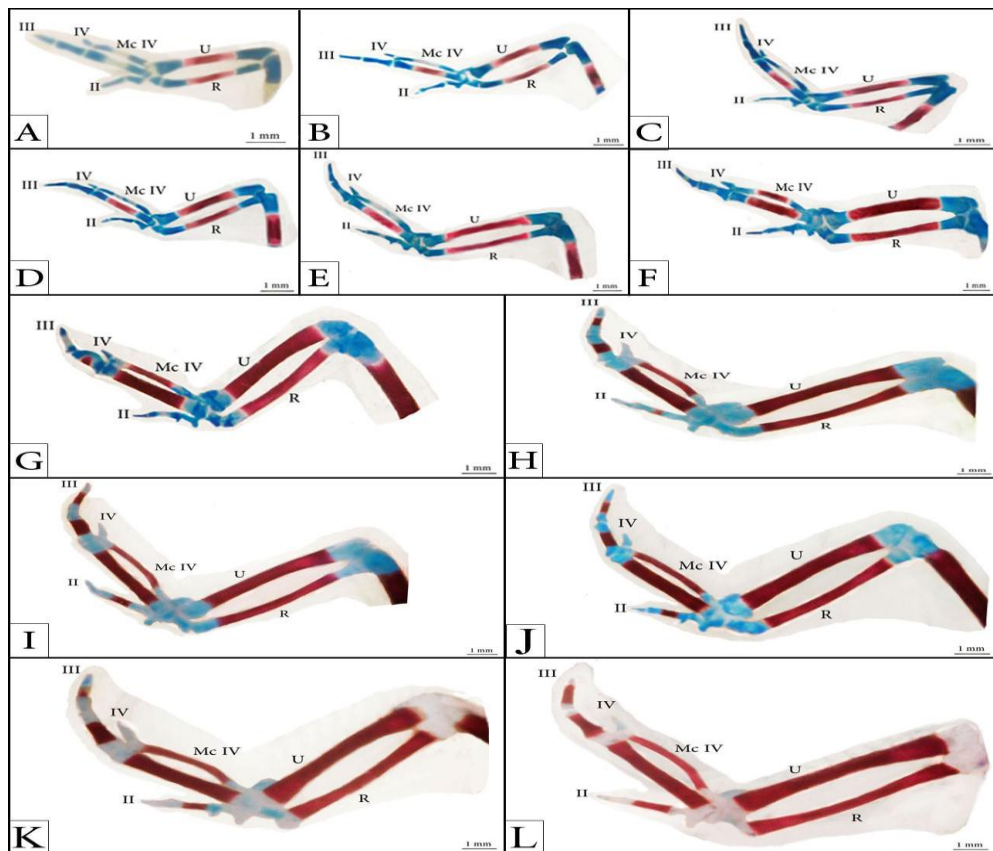


Figure 4: Series of Alcian Blue & Alizarin Red S – stained chick forelimb distal cartilaginous and bony elements at stages 34 – 36 (A – C) and 38 – 46 (D – L). II-IV, Digits II-IV respectively; Mc IV, Metacarpal IV; R, Radius; U, Ulna. Dorsal view. Scale bar = 1mm.

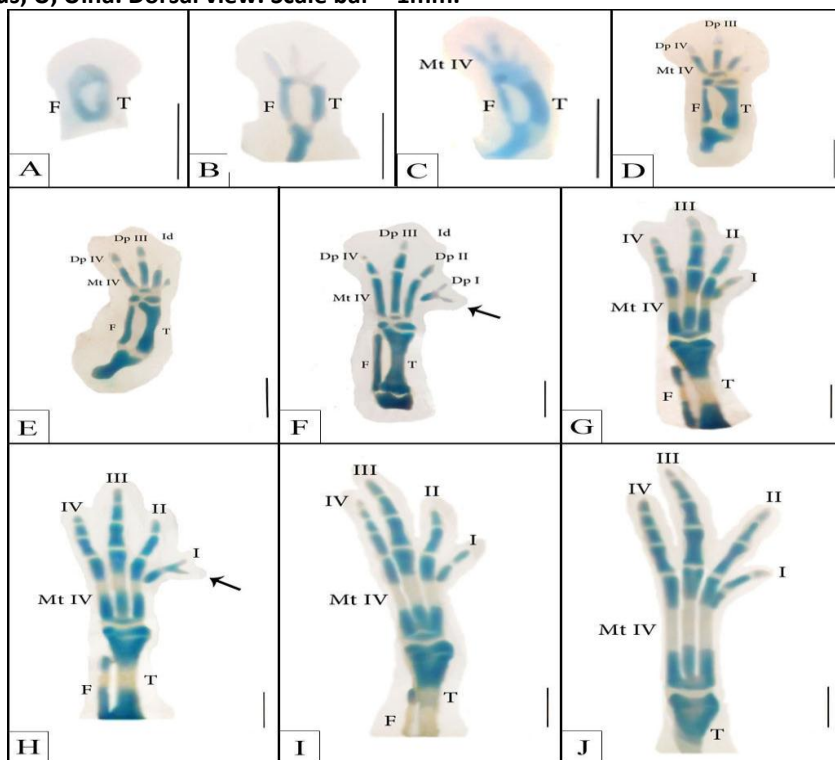


Figure 5: Series of Alcian Blue – stained chick hindlimb distal cartilaginous elements at stages 25 – 34 (A – J). Dp I-IV, Digit primordia I-IV respectively; F, Fibula; I-IV, Digits I-IV respectively; Id, Interdigital space; Mt IV, Metatarsal IV; T, Tibia. Arrows indicate the forked phalanx of the first toe. Dorsal view. Scale bar = 1mm.

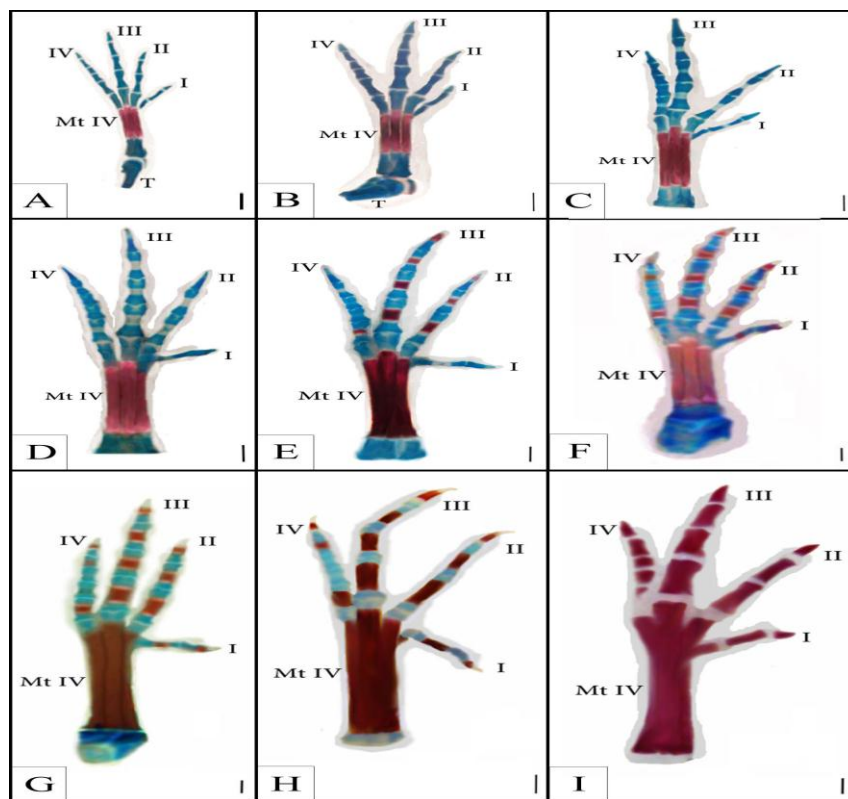


Figure 6: Series of Alcian Blue & Alizarin Red S – stained chick hindlimb distal cartilaginous and bony elements at stages 35 (A), 38 – 44 (B – H) and 46 (I). I-IV, Digits I-IV respectively; Mt IV, Metatarsal IV; T, Tibia. Dorsal view. Scale bar = 1mm.

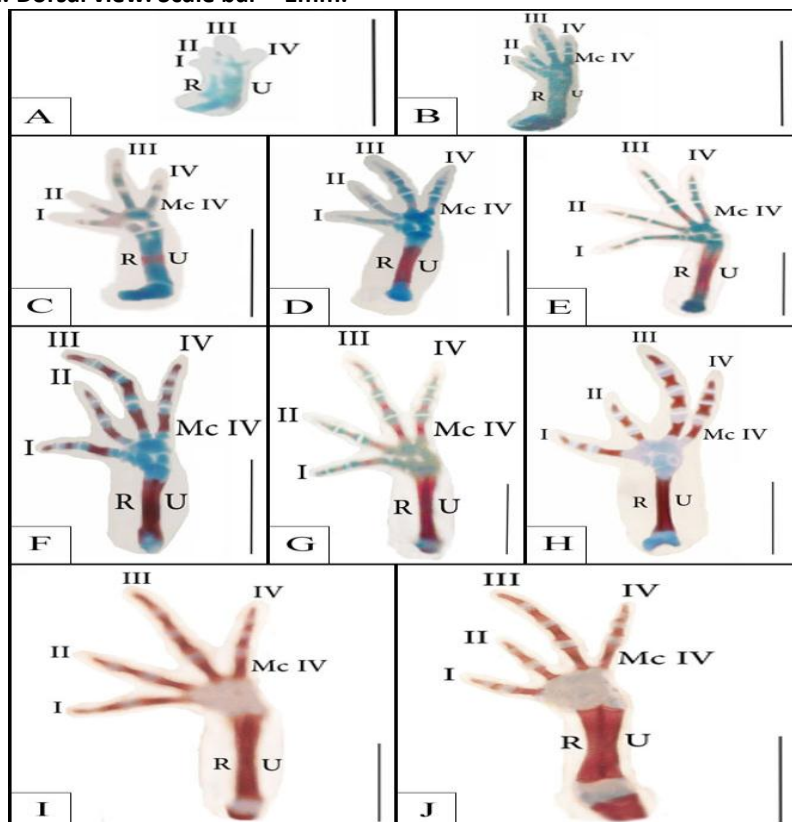


Figure 7: Series of single and double stained tadpole forelimb distal cartilaginous and bony elements at stages 55 – 60 (A – F) and 62 – 65 (G – J). I-IV, Digits I-IV respectively; Mc IV, Metacarpal IV; R, Radius; U, Ulna. Dorsal view. Scale bar = 1mm.

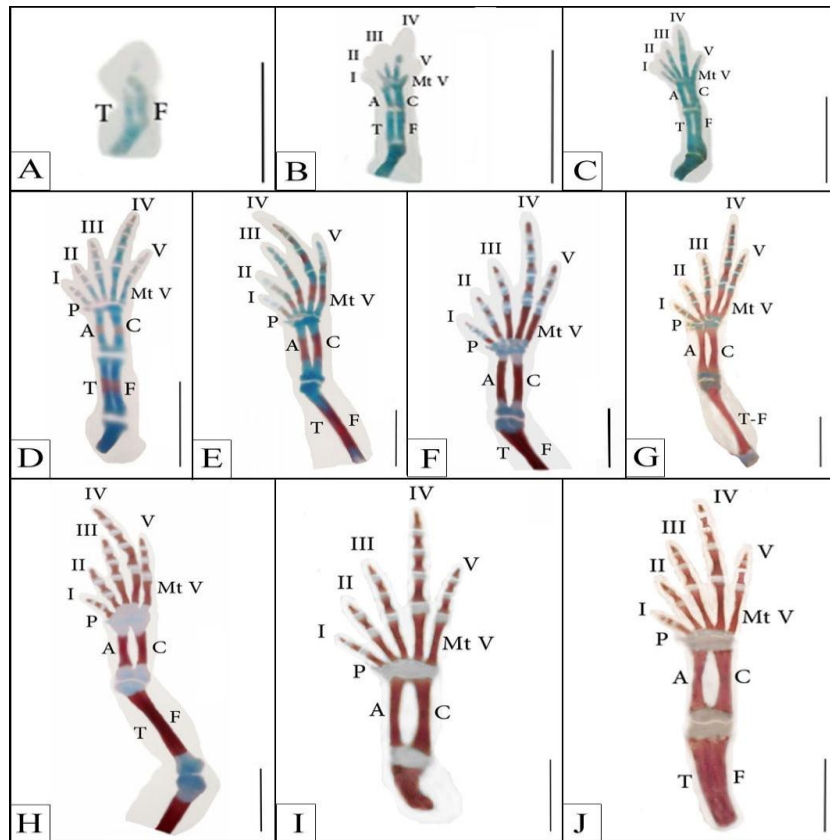


Figure 8: Series of single and double stained tadpole hindlimb distal cartilaginous and bony elements at stages 54 – 57 (A – D), 59 – 60 (E – F) and 62 – 65 (G – J). A, Astragulus; C, Calcaneum; F, Fibula; I-V, Digits I-V respectively; Mt V, Metatarsal V; P, Prehallux; T, Tibia; T-F, Tibio-fibula. Dorsal view. Scale bar = 1mm.

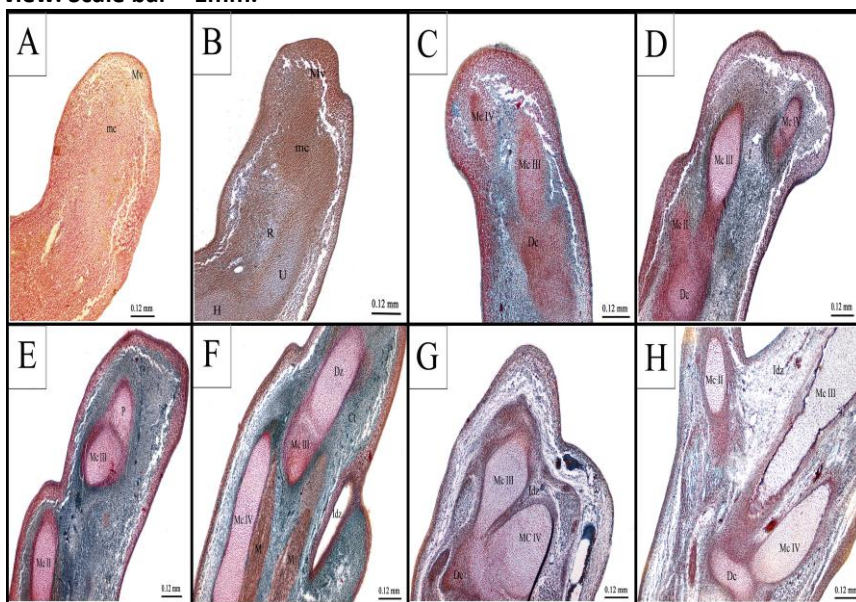


Figure 9: Photomicrographs of representative histological sections through the autopodium of the forelimbs of the chick stained with MTS. Stages 26 – 27 (A – B), 29 – 32 (C – F) and 34 – 35 (G – H). Ct, Connective tissue; Dc, Distal carpalia; Dz, Digital zone; H, Humerus; Idz, Interdigital zone; M, Muscle; mc, Mesenchyme condensataion; Mc II, III and IV, Metacarpal II, III and IV respectively; Mv, Marginal vein; P, Phalanx; R, Radius; U, Ulna. Scale bar = 0.12 mm.

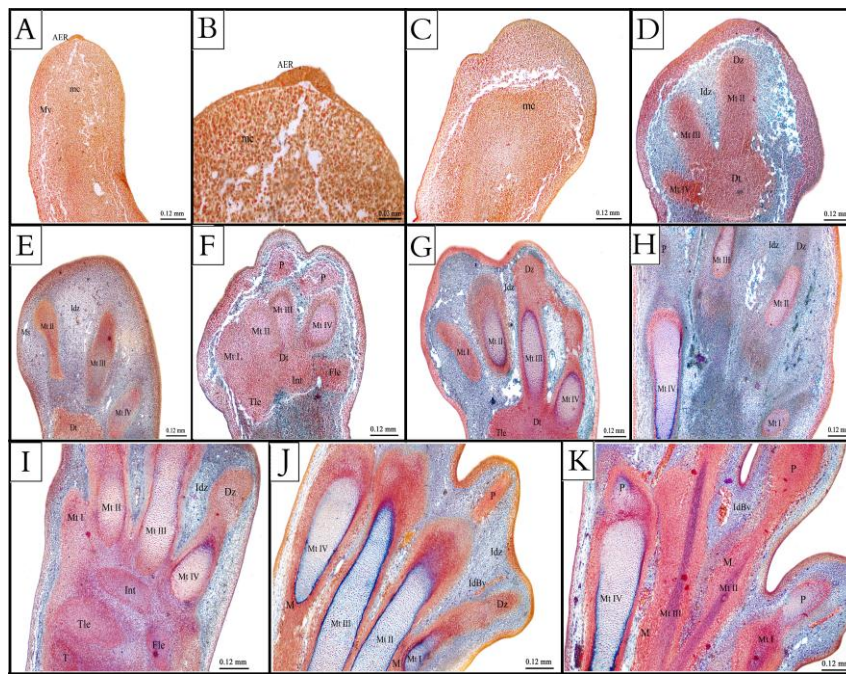


Figure 10: Photomicrographs of representative histological sections through the autopodium of the hindlimbs of the chick stained with MTS. Stages 25 (A&B), 26 – 29 (C – F), 30 (G&H) and 31 – 33 (I – K). AER, Apical ectodermal ridge; Dt, Distal tarsalia; Dz, Digital zone; Fle, Fibulare; IdBV, Interdigital Blood vessel; Idz, Interdigital zone; Int, Intermedium; M, Muscle; mc, Mesenchyme condensataion; Ms, Marginal sinus; Mt I, II, III and IV, Metatarsal I, II, III and IV respectively; Mv, Marginal vein; P, Phalanx; T, Tibia; Tle, Tibiale. Scale bar = 0.12 mm except B 0.03.

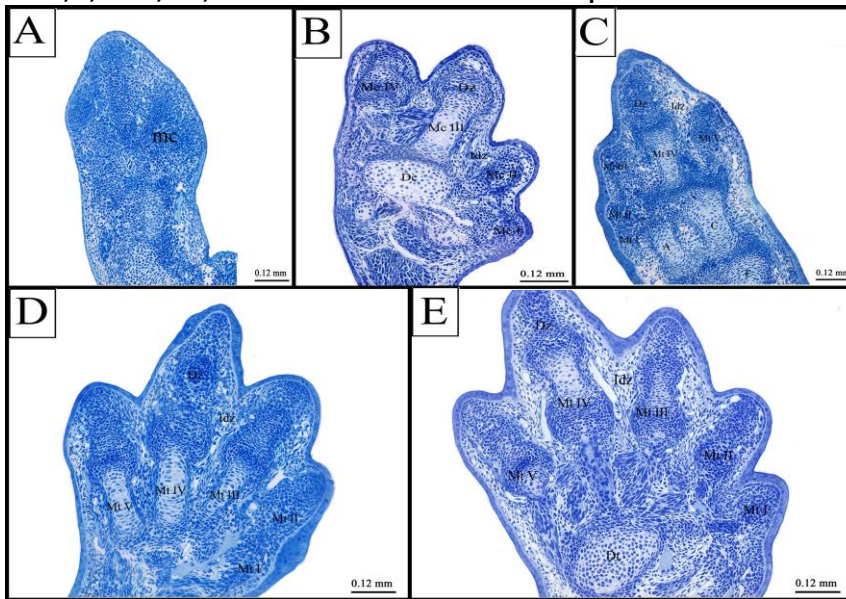


Figure 11: Photomicrographs of representative histological semithin sections through the autopodium of the forelimbs (A & B) and the hindlimbs (C, D & E) of the tadpole stained with TB. Stages 53 (A), 56 (B), 55 (C) and 56 (D&E). A, Astragulus; C, Calcaneum; Dc, Distal carpalia; Dt, Distal tarsalia; Dz, Digital zone; F, Fibula; Idz, Interdigital zone; mc, Mesenchyme condensation; Mc I, II, III and IV, Metacarpal I, II, III and IV respectively; Mt I, II, III, IV and V, Metatarsal I, II, III, IV and V respectively. Scale bar = 0.12 mm.

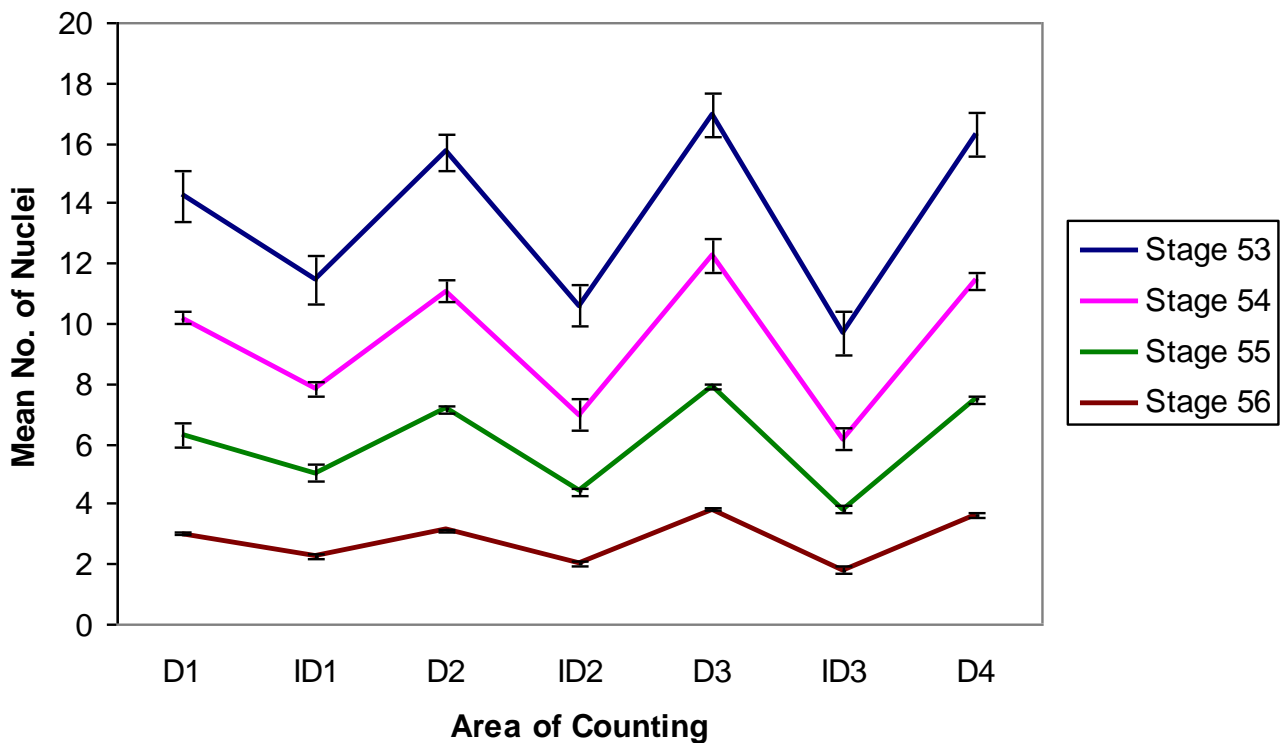


Figure 12: Graph showing differences in the mean number of nuclei in both digital (D) and interdigital (ID) areas in the autopodium of the forelimb of the developing toad *Bufo regularis*. Digits are indicated as D1, D2, D3 & D4.

Developmental Stage	Area of Counting						
	D1	ID1	D2	ID2	D3	ID3	D4
53	14.24 ± 0.88	11.48 ± 0.80*	15.72 ± 0.60**	10.60 ± 0.68**	16.96 ± 0.72**	9.69 ± 0.72**	16.32 ± 0.72**
54	10.20 ± 0.21	7.83 ± 0.24**	11.07 ± 0.36***	6.96 ± 0.51***	12.27 ± 0.54**	6.15 ± 0.36***	11.43 ± 0.30***
55	6.28 ± 0.38	5.02 ± 0.30**	7.16 ± 0.12***	4.42 ± 0.12***	7.88 ± 0.08***	3.82 ± 0.10***	7.46 ± 0.10***
56	3.00 ± 0.04	2.25 ± 0.11**	3.12 ± 0.03***	2.02 ± 0.07***	3.80 ± 0.04***	1.81 ± 0.14***	3.63 ± 0.06***

Table 1: Differences in the mean number of nuclei in both digital (D) and interdigital (ID) areas in the autopodium of the forelimb of the developing toad *Bufo regularis*. Digits are indicated as D1, D2, D3 & D4. Data are shown as mean ± SEM.

*** P < 0.0001, ** P < 0.03, *P < 0.05

DISCUSSION

Embryological descriptions of vertebrate limb development have documented the appearance of differentiated limb structures in sequence along the long axis. This process begins by forming a limb bud at the fated sites and as the buds elongate, cells in regions of the bud nearest to the body wall (proximal regions) begin to differentiate [7]. The mesenchymal cells in the limb bud aggregate into its central region and form cellular condensations for the

initiation of chondrogenesis [51]. Since mesenchymal condensation is formed to represent the prepattern, of the limb skeleton, the regulation of condensation size, shape and timing is important in the formation of the normal skeletal pattern [2, 7]. The process of condensation is affected by several cellular properties, such as motility and affinity [51], suggesting the importance of these properties for the cartilage pattern formation of the limb. Position-specific condensation indicates that mesenchymal cells in the limb bud possess distinct properties in a position-specific fashion. After pattern formation has been completed, limb buds stop growing out. However, the molecular mechanisms involved in the cessation of outgrowth and tip formation are not known [24]. Moreover, interdigital tissue has a high chondrogenic potential and this potential of interdigital tissue to form cartilage could account for the reported observation that interdigital cells contribute to digit condensations by cell migration [20, 52]. After the condensations have been established, digital rays elongate and periodically segment to form inter-phalangeal joints and thus, generate a precise number of phalanges. The formation of phalanges is a patterning process since the number of elements is characteristic of a particular digit according to its PA location. The mechanism of generation of phalanges in tetrapods is not well understood [24].

The AER is an essential signaling center governing vertebrate limb development [2, 3, 53]. The importance of the AER was demonstrated by classic experiments in chicken embryos showing that AER removal at progressively later stages of limb development causes a progressive loss of distal elements of the limb [54]. Although different models have been proposed to explain limb skeletal patterning along the PD axis, AER function in this process has remained largely unclear. For example, the progress zone (PZ) model postulates that the AER provides permissive signals to keep PZ cells labile until they exit the zone, at which time these cells are autonomously specified by ceasing to acquire 'positional information'. By contrast, the Early Specification (ES) model proposes that PD elements are specified rather than progressive at the earliest stages of limb bud development, and that the AER regulates subsequent expansion of progenitor pools by promoting cell proliferation and survival [55]. Furthermore, recent models suggest that PD elements are specified via dynamic interactions between the flank of the lateral plate mesoderm and the AER [56]. Like the situation in *Xenopus laevis* [57], the AER was formed at stage 51 of *Bufo regularis*, it persisted at stage 52 then it disappeared by stage 53 [58]. The present study demonstrated the presence of AER of the hindlimb of chick embryo at stage 25. However, stage 52 of the toad is out of the scope of the present study.

The early limb bud consists of a core of mesenchymal cells covered by an ectodermal jacket. In the course of development, the limb undergoes progressive outgrowth and at the same time, the skeleton differentiates in the mesodermal core of the bud [1, 9, 22]. Outgrowth is accomplished by the proliferation of the most distal segment of the mesoderm i.e. the PZ which is under the influence of AER. Members of the FGF family appear to be the signals produced by the AER to maintain the mesoderm of the PZ in an undifferentiated and proliferating stage [13-15, 59]. Differentiation of the mesoderm into the cartilaginous skeletal primordium of the limb begins proximally in the central core mesenchyme of the bud and progresses distally by the successive incorporation of cells leaving the PZ [54]. Concomitantly with the formation of skeletal cartilages, a considerable number of the remaining mesenchymal cells of the bud are eliminated by apoptotic cell death. This dying process takes place in a patterned fashion forming well defined areas of cell death which correlate with the limb phenotype of the different species [60]. The areas of interdigital cell death are found between

the developing digits of all amniote embryos [60]. Apoptotic cells were positively demonstrated in the interdigital mesenchyme by caspase-3 in case of the developing chick autopodium but there was no trace of these apoptotic cells in its tadpole counterpart using the same immunohistochemical technique (data not shown). Furthermore, investigating the ultrastructural changes in the interdigital areas within the developing chick autopodium revealed the presence of different stages of apoptosis (data not shown). Similarly, apoptosis has been observed in the interdigital spaces of many tetrapod species [25, 40, 61].

One of the major challenges in developmental biology is to understand how detailed anatomy is generated. The mechanism underlying formation of the paddle shape of the autopod presents a distinct puzzle, because it occurs relatively late during limb bud outgrowth, and is associated with preferential expansion of mesoderm along the PA axis relative to proximal regions [20]. Differences in the overall timing of developmental events during autopodium development in tetrapods may be attributed to different ecological and reproductive strategies. As the distal segment of the vertebrate limb, the autopod is characterized by the presence of digits, crucial elements for the function of the limb [7]. Evidence that each digit primordium has its own patterning mechanism comes from work mostly on chick leg development [62]. The latter showed that each individual digital ray is under the influence of immediately adjacent tissues and that its subsequent morphology can be altered independently of the other rays. Although the ossification of the phalanges occurs in a PD direction in several tetrapods including reptiles [63], each toe has a different number of phalanges [21].

The digits of the limb represent an obvious example of repeating structure. There has been much previous research on signals which pattern the developing chick wing, particularly on the establishment of PA polarity. It is now well established that sonic hedgehog (Shh) plays a pivotal role in controlling digit number and pattern [20, 22] but it is not clear which genes mediate the response to Shh signalling and encode AP positional information. It has been reported early that digit number is related to the width of the bud and this depends on the length of the AER [64]. Franssen et al. [65] reported significant differences in the way in which digits form even within amphibians. Fusion of elements occur at later stages and several condensations in the embryo can appear as a single bony element in adults, and this fact has led to different descriptions in the number of phalanges. There are only three digits in the chick wing, all with very distinct morphologies and numbered, from AP direction, II, III and IV although this numbering system has been the subject of much debate. Numerous studies suggest that, prior to the emergence of their morphological characters, the future digits are established in a pattern of positional values [37, 39, 66] within the mesoderm. A good model to avoid this uncertainty is the chicken leg which has the more typical tetrapod morphology and each toe has a different number of phalanges according to their position i.e. toe I (two phalanges), II (three), III (four) and IV (five). In all of these numberings the last phalanx or tip is included. A detailed morphometric analysis of the early condensation steps would help in our understanding of phalanges formation. Within the large scope of the present study, more investigations utilizing immunohistochemical and transmission electron microscopical techniques are currently underway (Badawy et al., in preparation).

Investigation of distal limb formation in chickens reveals that birds are no exception to this general pattern and sequence of digit formation and reduction. Examinations of digit

development reveal that the posterior most fully formed digit in the avian wing is located in the position of the primary axis indicating that it is in position 4, and thus the two anterior digits are inferred to be in positions II and III. This finding has been confirmed by studies staining the early digit condensations. Early investigations of digit condensation [67] revealed only four digits condensations; however, because these techniques require extracellular matrix resulting from chondrification, these techniques neglect transient digit anlagen that appear early in development before chondrification. More recently, techniques that visualize the initial condensation of prechondrogenic cells reveal five digit anlagen in the developing avian wing reviewed in [68]. Several independent research groups using distinct techniques including documentation of capillary degeneration associated with cell condensation [69] provided strong evidence that the digits of the avian wing develop in positions II, III and IV [39]. In amphibians, the progression of digit morphogenesis follows a specific pattern that differs from other tetrapods, where individual digits emerge sequentially from the limb palette during normal development but not regeneration [70]. The individualization of digits appears therefore to result from growth and elongation of the digits rather than by the apoptosis of the preformed interdigital tissue. During limb development in tadpoles, digits emerge from the limb palette in a sequential manner; digits IV and III are the first to grow out, followed by digits II and I. Determination of the cell density in the digital and interdigital areas of the toad in the present study confirm that the digits emerge sequentially from the limb palette especially that no apoptotic cells were detected in the interdigital areas of the developing autopodium of the toad (Badawy et al., in preparation).

The finding that the autopodium of both chick and tadpole develops in a PD direction is in agreement with other investigated vertebrates except salamanders [36]. We noted that skeletal development in the proximal portion of the autopodium in the investigated developmental stages is clearly more advanced than that further distally. This is in line with the PD sequence of development in the limb first demonstrated by Saunders [71] for the chick and by Tschumi [17] for Xenopus. The histological findings of the present study confirmed the whole mount investigation in terms of both PD and PA axial directions. However, our results indicated that the tadpole of the toad *Bufo regularis* forms limbs in a different way compared to the chick *Gallus domesticus*. Indeed, the chick limb development is more similar to amniote limb development than to that of the anamniote toad. This study is in accordance with the findings of [72] conducted on salamander in that the hindlimb lags behind the development of the forelimb in the chick while both limbs exhibited the same level of development in terms of ossification in case of the toad. It is generally accepted that the hindlimb lags behind the development of the forelimb [27]. However, except for specific aspects, morphogenetic processes in the fore- and hindlimbs are generally similar. The most significant distinction between the developing limb of the chick and the toad is the outgrowth of the digits. In both species the limb bud extends from the body wall and continues to lengthen distally as the precartilage foci of the humerus, radius, and ulna begin to condense (own observations). The timing of digit appearance varies between the two species. In the tadpole, each digit extends from the limb bud as its own individual bud without apoptosis (Badawy et al., in preparation). Within each bud, the metapodials and phalanges condense and segment from one another. These internal processes of cartilage formation are coincident with the elongation of the digital bud. The developing amphibians also differ with regard to the sequence of digit condensation [36]. In *Ambystoma mexicanum*, Digit II begins to form first, followed by Digits I, III, and IV. This is not in accordance with the sequence of digitation in both investigated models of the present

study where digitations occurred in a PA direction. These differences in timing of cartilaginous condensation certainly indicate variation in the timing or location of gene expression. Exploration of genes such as Shh and Sox9 could greatly enhance our understanding of how digit condensation is triggered [16].

It can be concluded that although morphogenetic processes in the fore- and hindlimbs are generally similar within tetrapods, species differences do exist and therefore limb development is variable as the present study demonstrated. Consequently, concepts that frame the basis for the tetrapod model of limb development, things that are often taken for granted that limb development proceeds in a PD direction that digits form in a PA direction, that cell death occurs during digit formation are not even true for all groups of tetrapods. Evolution of specialized life history modes within tetrapods has involved novel disassociations among the sequence of cartilage condensation, digit elongation, and the utilization of interdigital spaces. Further study of the developmental programs of tetrapod limbs will likely reveal a link between developmental biology, ecology, and evolution [73-76].

Conflict of interest statement

We declare that we have no conflict of interest.

REFERENCES

- [1] Tickle C. *Int J Dev Biol* 2000; 44: 101-108.
- [2] Capdevila J, Izpisua-Belmonte J. *Annu Rev Cell Dev Biol* 2001; 17: 87-132.
- [3] Niswander L. *Nat Rev Genet* 2003; 4: 133-143.
- [4] Talamillo A, Bastida M, Fernandez-Teran M, Ros M. *Clin Genet* 2005; 67: 143-153.
- [5] Tickle C, Munsterberg A. *Curr Opin Genet Dev* 2001; 11: 476-481.
- [6] Tickle C. *Nature Reviews, Molecular Cell Biology* 2006; 7: 45-53.
- [7] Cole A. *Aeugr Ocpoelaen Cells And Materials* 2011; 21: 122-129.
- [8] Ohuchi H, Nakagawa T, Yamamoto A, Araga A, Ohata T, Ishimaru Y, Yoshioka H, Kuwana T, Nohno T, Yamasaki M, Itoh N, Noji S. *Development* 1997; 124: 2235-2244.
- [9] DeLise A, Stringa E, Woodward W, Mello M, Tuan R. *Methods Mol Biol* 2000; 137: 359-375.
- [10] Olsen B, Reginato A, Wang W. *Annu Rev Cell Dev Biol* 2000; 16: 191-220.
- [11] Niswander L, Martin G. *Development* 1992; 114: 755-768.
- [12] Niswander L, Jeffrey S, Martin G, Tickle C. *Nature* 1994; 371: 609-612.
- [13] Fallon J, Lopez A, Ros M, Savage M, Olwin B, Simandl B. *Science* 1994; 264: 104-107.
- [14] Mahmood R, Bresnick J, Hornbruch A, Mahony C, Morton N, Colquhoum K, Martin P, Lumsden A, Dickson C, Mason I. *Curr Biol* 1995; 5: 797-806.
- [15] Vogel A, Rodriguez C, Izpisua-Belmonte J. *Development* 1996; 122: 1737-1750.
- [16] Fernandez-Teran M, Ros M. *Int J Dev Biol* 2008; 52: 857-871.
- [17] Tschumi P. *Journal of Anatomy* 1957; 91: 149-172.
- [18] Gerlach J. *Sci Res* 2012; 7: 1083-1099.
- [19] Tickle C. *Dev Cell* 2003; 4: 449-458.
- [20] Stricker S, Mundlos S. *Developmental Dynamics* 2011; 240: 990-1004.
- [21] Mackie E, Tatarczuch L, Mirams M. *J Endocrinol* 2011; 211: 109-121.
- [22] Towers M, Tickle C. *Development* 2009; 136: 179-190.

- [23] Wada N. *Developmental Dynamics* 2011; 240: 969-978.
- [24] Sanz-Ezquerro J, Tickle C. *J Anat* 2003; 202: 51-58.
- [25] Sato K, Seki R, Noro M, Yokoyama H, Tamura K. *J Exp Zool (Mol Dev Evol)* 2010; 314B: 539-551.
- [26] Shubin N, Alberch P. *Evol Biol* 1986; 20: 319-387.
- [27] Sawad A, Hana B, Al-Silawi A. *International Journal of Poultry Science* 2009; 8: 710-714.
- [28] Hall B, Miyake T. *Bioessays* 2000; 22: 138-147.
- [29] Kronenberg H. *Nature* 2003; 423: 332-336.
- [30] Ferguson C, Miclau T, Hu D, Alpern E, Helms J. *Ann N Y Acad Sci* 1998; 857: 33-42.
- [31] Colnot C, Helms J. *Mech Dev* 2001; 100: 245-250.
- [32] Ballock R, O'Keefe R. *J Bone Joint Surg Am* 2003; 85-A: 715-726.
- [33] Provot S, Schipani E. *Biochem Biophys Res Commun* 2005; 328: 658-665.
- [34] Wagner E, Karsenty G. *Curr Opin Genet Dev* 2001; 11: 527-532.
- [35] Tickle C, Eichele G. *Annu Rev Cell Biol* 1994; 10: 121-152.
- [36] Fröbisch N, Shubin N. *Developmental Dynamics* 2011; 240: 1087-1099.
- [37] Wolpert L. *Int J Dev Biol* 2002; 46: 869-870.
- [38] Wolpert L. *Trends Genet* 1996; 9: 364-359.
- [39] Young R, Bever G, Wang Z, Wagner G. *Developmental Dynamics* 2011; 240: 1042-1053.
- [40] Chen Y, Zhao X. *The J Exp Zool* 1998; 282: 691-702.
- [41] Feduccia A. *Trends Ecol Evol* 2001; 16: 286-285.
- [42] Galis F, Kudrát M, Metz J. *Hox Genes. J Exp Zool (Mol Dev Evol)* 2005; 304B: 198-205.
- [43] Vargas A, Fallon J. *J Exp Zool (Mol Dev Evol)* 2005; 304B: 206-219.
- [44] Welten M, Verbeek F, Meijer A, Richardson M. *Evolution & Development* 2005; 7(1): 18-28.
- [45] Hamburger V, Hamilton H. *Embryo J Morphol* 1951; 88: 49-92.
- [46] Sedra S, Michael M. *Cesk Morf* 1961; 9: 333-351.
- [47] Korn M, Cramer K. *J Vis Exp* 2007; (8), e306.
- [48] Cortés-Delgado N, Pérez-Torres J, Hoyos J. *Int J Morphol* 2009; 27: 1163-1167.
- [49] Pramod K, Vaswani V, Bindhu S. *Recent Research In Science and Technology* 2011; 3: 54-58.
- [50] Humason G. *Animal Tissue Techniques*. 4th edn., Freeman, W. Co., San Francisco, 1979.
- [51] Hall B, Miyake T. *Int J Dev Biol* 1995; 39: 881-893.
- [52] Omi M, Sato-Maeda M, Ide H. *Int J Dev Biol* 2000; 44: 381-388.
- [53] Martin G. *Genes Dev* 1998; 12: 1571-1586.
- [54] Summerbell D. *J Embryol Exp Morph* 1974; 32: 227-237.
- [55] Dudley A, Ros M, Tabin C. *Nature* 2002; 418: 539-544.
- [56] Tabin C, Wolpert L. *Genes Dev* 2007; 21: 1433-1442.
- [57] Tarin D, Sturdee A. *J Embryol Exp Morph* 1971; 26: 169-179.
- [58] Abdel-Karim A, Michael M. *Qatar Univ Sci J* 1991; 11: 285-298.
- [59] Niswander L, Tickle C, Vogel A, Booth I, Martin G. *Cell* 1993; 75: 579-587.
- [60] Hurlé J, Ros M, Garcia-Martinez V, Macias D, Gañan Y. *Scan Microsc* 1995; 9: 519-534.
- [61] Chang H, Tse Y, Kaufman M. *J Anat* 1998; 192: 59-72.
- [62] Dahn R, Fallon J. *Science* 2000; 289: 438-441.
- [63] Lima F, Vieira L, Santos A, Pereira H, De Simone S, Hirano L, Romão M, Silva J, Coutinho M. *J Morphol Sci* 2011; 28: 4-10.
- [64] Brickell P, Tickle C. *Bioessays* 1989; 11: 145-149.
- [65] Franssen R, Marks S, Wake D, Shubin N. *Journal of Morphology* 2005; 265: 87-101.

- [66] Wolpert L, Beddington R, Brockes J, Jessell T, Lawrence P, Meyowitz E. Principles of Development. Oxford & University Press 1998.
- [67] Burke A, Feduccia A. Science 1997; 278: 666-668.
- [68] Wagner G. Theory Biosci 2005; 124: 165-183.
- [69] Kundrát M. J Exp Zool (Mol Dev Evol) 2009; 312: 30-41.
- [70] Vlaskalin T, Wong C, and Tsilfidis C. Dev Genes Evol 2004; 214: 423-431.
- [71] Saunders J. Jr. J Exp Zool 1948; 108: 363-404.
- [72] Fröbisch N. Biol Rev 2008; 83: 571-600.
- [73] Hinchliffe J. Development Supplement, 1994; 163-168.
- [74] Hinchliffe J. Int J Dev Biol 2002; 46: 835-845.
- [75] Mabee P. Amer Zool 2000; 40:789-800.
- [76] Gardiner D, Torok M, Mullen L, Bryant S. Amer Zool 1998; 38:659-671.